This article has been published in Metallurgical and Materials Transactions A. The final publication is available at Springer via https://doi.org/10.1007/s11661-015-2990-5 .

An innovative two-stage reheating process for wrought aluminum alloy during thixoforming

Abstract

An innovative two-stage reheating process has been developed to improve the thixotropic behavior of semi-solid wrought aluminum alloy during thixoforming. The variation of the microstructural evolution mechanisms with temperature and holding time during a traditional process and two-stage reheating process are investigated in this paper. A desirable semi-solid microstructure with spherical-like grains surrounded by a uniform liquid film is obtained in the two-stage reheating process. The semi-solid microstructure obtained via this two-stage reheating process has more refined equivalent diameters, a better spherical degree, a lower coarsening rate constant of solid grains and a reduced possibility of defects caused by entrapped liquid than that produced by the traditional reheating process. These results prove that the two-stage reheating process is a promising method for manufacturing wrought aluminum alloy during thixoforming.

Keywords: wrought aluminum alloy; two-stage reheating process; semi-solid microstructure; thixoforming

1. Introduction

Thixoforming, a typical method for the semi-solid processing of aluminum alloys, includes three procedures: semi-solid billet preparation, reheating and forming[1]. The desirable prepared material for thixoforming is a partially remelted semi-solid billet with a suitable volume fraction in which the micro solid particle exhibits as almost spherical shape[2]. This technique offers practical advantages over traditional forging and casting, including minimal splashing, high production efficiency, and a reduction of porosity and forming force. Thixoforming process can be used for a wide range of applications due to the favorable quality of the resulting products [3-5]. The key point of thixoforming is the formation of a non-dendritic microstructure during the reheating process at temperatures between the solidus and liquidus, which remarkably affects the subsequent forming process as well as the mechanical properties of the finished product.

The constitutive behavior of a material during thixoforming is complex, and varies

from solid-like character to liquid-like character depending on the shear rate [6-7]. The metal must flow enough to fill a mold, but must also have enough strength to allow the semi-solid slug to maintain its shape under its own weight while it is being transported. Obviously, the reheating process prior to the forming stage plays a major role in achieving favorable thixotropic behavior during thixoforming. The corresponding grain morphology must be non-dendritic with the solid and liquid phases must be uniformly distributed throughout the semi-solid state [8].

Although thixoforming is currently used as a commercial process, it has only found real success with Al–Si casting aluminum alloys such as A356 and A357, with strengths between 220–260 MPa and 8–13% elongation [6]. The large eutectic fractions of these alloys aids in the production of the desirable non-dendritic grain morphology in the semi-solid state. At present, there is significant interest in developing the thixoforming process for the production of high-performance wrought aluminum alloys. One of the challenges of casting alloys during thixoforming is grain coarsening. Atkinson and Liu [7] have shown that for wrought alloys, the presence of precipitates and dispersoids at grain boundaries interferes with the migration and diffusion of the liquid film, particularly for thin liquid films between spheroids, and hence inhibits coarsening. However, casting aluminum alloys do not normally have such particles present to help prevent coarsening. Thus, the reheating parameters, such as the holding time in the semi-solid state, must be restricted to avoid an excessively coarse microstructure. It is well-known that thixoforming is proved to be a potential commercial manufacturing route for the 6061 wrought aluminum alloy, although further research must be undertaken in order to develop a detailed understanding of the effect of reheating parameters on microstructure. The 6061 alloy has been widely used in military, aerospace and automotive applications because of its lightweight and excellent mechanical properties.

The goal of thixoforming is to produce fine and spherical-like microstructures with an appropriate liquid fraction, which will greatly facilitate the thixoforming process. Herein, the effect of a two-stage reheating process on the microstructural evolution of 6061 is investigated. First, various annealing options are tested in order to determine the optimal reheating temperatures. Second, the evolution mechanisms of the semi-solid spherical-like microstructure are explored in order to optimize the industrial process. Alloy properties such as the equivalent diameter and roundness of the solid globules, the coarsening rate, and the fraction of entrapped liquid and how

they change with the reheating temperatures are discussed.

2. Optimization of a two-stage reheating process

A two-stage reheating process is proposed in order to achieve a balance between grain spheroidization, holding time, and coarsening during the reheating process.

2.1. Materials

A commercially available 6061 wrought aluminum alloy is investigated; its chemical composition is given in Table 1. The composition is measured by photoelectric direct reading spectrometry (PMI-MASTER PRO, Oxford Instruments).

2.2. Methods

Sample Preparation: First, a 500 mm diameter billet is cast using near-liquidus semi-continuous casting method. An example of the initial non-dendritic microstructure is shown in Fig. 1. Then, small samples with dimensions of 15 mm ×15 mm ×15 mm are machined for the reheating experiments.

Reheating Equipment: An isotemp muffle furnace (Fisher Scientific 550-126) was used for the heating process, which can provide PID microprocessor temperature control at operating temperatures from 323 to 1398 K. A wall heater and floor heater are used together to maintain uniform heating. The average temperature stability is +/- 1 K.

Reheating Experiments: A series of two-stage reheating experiments is carried out to find the optimum reheating process for the promotion of the desired non-dendritic microstructure. In total, six different heating routes are assessed, as shown in Fig. 2. The solidus and liquidus temperatures are defined as T_S and T_L, respectively. Three of the tests utilized a stage-one temperature near T_S – 10 K, T_S, and T_S + 10 K: 845, 855, and 865 K (i.e. T_S – 10 K, T_S, and T_S + 10 K) , the other three tests utilize a stage-one temperature near T_L : 918,928 and 938 K(i.e. T_L – 10 K, T_L, and T_L + 10 K). The temperature of the second stage is 907 K, corresponding to a liquid fraction of 0.2.

The reheating procedure for a typical sample is as follows. First, the sample is placed into a furnace that has been previously preheated to the desired stage-one temperature. After 5 minutes, the furnace and sample are heated (or cooled) to the stage-two

temperature at a heating (or cooling) rate of 10 K/min. Once the stage-two temperature is reached, the sample is held at that temperature for an additional 15 minutes. Finally, the sample is quenched in water to preserve the microstructure from the semi-solid state.

Microstructural Analysis: After quenching, the samples are ground, polished and then etched in a mixed acid solution of 2 ml HF, 3 ml HCl, 5 ml HNO_3, and 190 ml H_2O. Optical microstructure investigations are then carried out.

2.3. Results

The solidus (855 K) and liquidus (928 K) temperatures of this alloy were measured by differential scanning calorimetry (DSC). The relationship between the temperature and liquid fraction for 6061 wrought aluminum alloy is measured by DSC, as depicted in Fig. 3. As can be seen, the liquid fraction is 0.2 at 907K.

The 6061 aluminum alloy samples are heated to near T_S for the first stage and then to 907 K for the second stage. The results are shown in Fig. 4. As can be seen in Fig. 4(a), irregular grain shapes with some entrapped liquid can be observed for the 845 K → 907 K heating cycle. In this cycle, the first stage was at a temperature just below T_S and thus all of the alloying elements accumulate in the solution, making the structure uniform and stable. Liquid films form in regions of high alloy content, due to localized remelting. However they are not continuous, making no contribution to the spheroidization of the non-dendritic structure. Figure 4(b) shows the microstructure after the 855 K → 907 K heating cycle. During this test, the first stage is maintained at T_S. It can be seen that the solid grains are nearly spherical and uniformly distributed and most of the liquid is also distributed at the grain boundaries. Figure 4(c) shows the characteristics of microstructure after the 865 K → 907 K heating cycle. Here, the grains are non-uniform in size, and a considerable amount of entrapped liquid appears during the reheating process. As we explained above, it turns out that the significant differences between Fig. 4(b) and 4(c) is the variation of homogeneity of the solid grain size and the amount of intragranular liquid droplets entrapped inside the solid grains.

In the second series of experiments, the 6061 aluminum alloy samples are heated to near T_L for the first stage and then to 907 K for the second stage, which can be seen in Fig. 5. In all three micrographs, evidence of significant coarsening and grain growth is

present because the liquid provides a faster path for diffusion [8-9] as compared to the solid. In Fig. 5(a), it can be seen that the microstructure is filled with large intragranular liquid droplets and over-sized irregular solid grains for the samples treated at the lowest stage one temperature (i.e., 918 K). This phenomenon is mainly because the first-stage reheating temperature is 10 K below T_L, at this temperature, the solid phase cannot fully melt and large amounts of the liquid will trapped inside of the unmelted solid phase during the solidification process when the temperature is decreased to the final reheating temperature. Therefore, it can be seen that the liquid fraction is much higher in Fig. 5(a) (first stage at 918K) than in Fig. 5(b) (first stage at 928K). With an increase in the first-stage temperature to 928 K (i.e. T_L), the same trends are seen but they are less pronounced because the solid is almost fully liquid. As shown in Fig. 5(b), the solid grains are excessively coarsened, and regions of liquid segregation are visible both at the grain boundaries and inside the grains. Finally, when the sample is heated at the first stage to a temperature above T_L (i.e. 938 K), a tiny dendritic microstructure has formed among the big solid grains once the temperature is decreased to the final reheating temperature, which can be seen in Fig. 5(c). This microstructure will affect the homogeneous distribution of the solid and liquid phases and significantly decrease the thixotropic behavior during forming.

In general, the microstructure formed in the two-stage reheating procedure show better characteristics when they are formed near T_S compared to when they are formed near T_L. A desirable semisolid microstructure with fine and uniform spheroidal grains is shown in Fig. 4(b). Thus, in cycle 2, the mass is held at the solidus state for 5 minutes, and then is heated to a temperature that promotes a liquid fraction of 0.2 (907 K) for another 15 min. The experimental results show that an optimal microstructure for thixoforming of 6061 is formed using this procedure. For this sample, the grains are nearly spherical with a minimal amount of entrapped liquid.

3. Evolution mechanism of semi-solid microstructure

The results presented in Section 2 indicate that a novel two-stage reheating process for 6061 wrought aluminum alloy billets provides an optimal microstructure for thixoforming. In this section, the choice of the second-stage temperature is investigated to explore the evolution mechanisms of the semi-solid microstructure during reheating process. The results are compared to those of the traditional reheating process.

3.1 Methods

Two-stage process: Additional samples are reheated using the two-stage process introduced above. As shown in Fig. 6, at the first stage, samples are reheated to T_S =855 K and held at that temperature for 5 min. Then, the samples are heated to 893, 903, or 913 K for another 5 min. These temperatures correspond to liquid fraction of 0.07, 0.15, and 0.3, respectively. Afterward, the samples are held at temperature for additional 20, 25 and 30 min. In total, 9 samples are processed using this new two-stage method.

Traditional process: For the traditional method, samples are reheated to 893, 903, or 913 K in an electrical resistance furnace, and then are quenched after holding for 20, 25, and 30 min. In total, 9 samples are processed using the traditional method.

Analysis Techniques: Optical metallography is performed on all samples using Image Pro Plus. Specifically, the grain perimeter, non-entrapped liquid fraction, grain size and grain shape are quantified. The average grain size and shape are estimated based on the concepts of equivalent diameter (D_{eq}) and roundness (F) using Eq. (1) and (2)[8-11]

$$D_{eq} = \frac{1}{N}\sum_{N=1}^{N}\sqrt{\frac{4A_N}{\pi}} \tag{1}$$

$$F = \frac{1}{N}\sum_{N=1}^{N}\frac{4\pi A_N}{P_N{}^2} \tag{2}$$

where A_N, P_N and N denote the area, perimeter and the number of solid grains, respectively. Note that if the value of F is equal to 1, the solid grain is perfectly round.

The value of the non-entrapped liquid fraction ranges from 0 to 1, with a value of 1 corresponding to the scenario where there are no liquid droplets inside the solid grains. For thixoforming, this scenario is ideal since a high content of entrapped liquid may result in the occurrence of defects, such as shrinkage porosity during the subsequent forming and solidification of the thixoformed component.

Using the knowledge gained from quantifying the microstructures, the coarsening kinetics during the various reheating cycles is determined based on Eq. (3) [12-16]

$$D_{eq}^{\ 3} - D_{eq0}^{\ 3} = Kt \tag{3}$$

where D_{eq} is the equivalent diameter of a solid grain at the holding time t, D_{eq0} is the initial equivalent diameter at $t = 0$ (when temperature is constant), and K is the coarsening rate constant. The semi-solid grains at a holding time of 20 min under different temperatures are assumed to have equivalent diameters equal D_{eq0}, and thus they are used for the calculation of the coarsening rate.

3.2 Results and discussion

Figure 6-8 show a comparison of the microstructure obtained from the traditional reheating process at three different temperatures, i.e., 893 K (Fig. 7), 903 K (Fig. 8), and 913 K (Fig. 9), and from the two-stage reheating process with the first reheating stage set to $T_{S=}$ 855 K. The traditional reheating microstructures are shown in (a1), (b1), and (c1) of each figure, while the two-stage microstructures are given in (a2), (b2), (c2) of each figure. A number of general qualitative results can be obtained. First, the features shown in Fig. 7 (a2), Fig. 8 (a2) and Fig. 9 (a2) can occur due to either the partial wetting of the boundaries during the holding time, or due to the initial stages of grain coalescence. *A* represents some incomplete (or very thin) grain boundaries. From these micrographs, it is difficult to determine which of these causes most likely happens [9]. Second, as the holding time increases, grain growth will occur through gradual agglomeration of solid grains. Examples are marked as *O* in Fig. 6-8. At low and moderate solid fraction, where large drops of liquid aggregate at the solid grain boundaries, there exist some very small solid grains suspended in the liquid, in these conditions, coalescence can easily occur as adjacent grains can move and rotate until they share a common crystallographic orientation [17]. Third, as the holding time is further increased, Ostwald ripening occurs with large grains growing at the expense of smaller ones. This is indicated by the one-way red arrow in Fig. 6-8. It can also be seen that some grains form into large clusters, marked as “C” in Fig. 6-8. These are likely to contain entrapped liquid due to the agglomeration process, labeled as “I” in Fig. 6-8.

The local area of the grain boundary is partially remelted at a relatively low reheating temperature and short holding time. The microstructure formed by traditional

reheating Fig. 7 (a1) exhibits convoluted grain shapes with ambiguous boundaries, which may inherited from the slurry-prepared billets. On the other hand, the microstructure formed by two-stage reheating has indistinct near-spherical solid grains of an early form, as shown in Fig. 7 (a2). Grain boundaries are gradually penetrated by liquid due to the more eutectic structures become liquid as the holding time extends to 25 min. Free liquid aggregate at the grain boundaries with small grains suspended in the traditional reheating microstructure and an irregular rosette microstructure, as shown in Fig. 7 (b1), entraps a number of tiny liquid droplets. For the two-stage reheating microstructure Fig. 7(b2), less liquid is entrapped inside the solid grains, coalescence generally occurs with much clearer and smoother grain boundaries, and solid grains retain their irregular polygonal structure. The distribution of the liquid film is inhomogeneous and discontinuous. As shown in Fig. 7(c1), grains coarsen with increased holding time and some of the grain boundaries disappear as liquid droplets form inside the solid phase. The grain size is larger, and the distribution of the solid and liquid phase is less uniform than that of two-stage, as seen in Fig. 7(c2). The presence of some relatively large grains and large drops of entrapped liquid lead to undesirable mechanical properties.

The different semi-solid microstructural evolution of 6061 wrought aluminum alloy at 903 K during the two reheating processes is depicted in Fig. 8. The traditional reheating microstructures are shown in Fig. 8 (a1), (b1), and (c1), while the two-stage microstructures with the first reheating at solidus temperature of 855 K for 5 min are shown in Fig. 8 (a2), (b2), and (c2).

Higher temperature promotes the formation of a liquid film and a solid boundary fully penetrated by liquid in a shorter time. The existence of the liquid reduces the friction, which is beneficial to the spheroidization and rearrangement of solid grains. The microstructure formed by traditional reheating at a 20min holding time Fig. 8(a1) has a large amount of small liquid entrapped inside solid grains with clear grain boundaries; on the other hand the microstructure of the two-stage reheating Fig. 8 (a2) has partly spherical grains with diverse grain sizes. When holding time is extended to 25 min, distinct grain boundaries occur due to more remelted eutectic structure. The thickness of the liquid film is non-uniform and the shape of the solid grains is anomalous for the microstructure formed by traditional reheating, as shown in Fig. 8 (b1). The increased holding time leads to more convexity or high curvature. Therefore, parts of polygonal grains first remelt under the surface tension. Individual polygonal

grains separate by the liquid film due to the high interfacial energy of eutectic liquid phase. As shown in Fig. 8(b2), solid grains are polyhedral but do not display sharp corners. The two-stage reheating microstructure is comprised of fine and spherical-like polygonal grains with a homogeneously distributed thin liquid film along the grain boundaries, which is suitable for thixoforming. It is also observed that almost perfect globular grains are much more homogeneously distributed than in the case of the traditional reheating microstructure. As holding time continues, excessively coarse solid grains and some relatively large intragranular liquid pools are observed in the semi-solid microstructure, especially for the traditional reheating microstructure Fig. 8 (c1). The intragranular liquid droplets possibly originate from the internal inhomogeneity of the primary solid, which is caused by chemical segregation [18]. This entrapped liquid does not contribute to flow or participate in deformation, which may produce shrinkage and other defects during the solidification process. These relatively large grains and intragranular liquid droplets have an adverse effect on the final mechanical properties of the semi-solid products, as shown in Fig. 8 (c1) and (c2).

Figure 9 depicts the temporal evolution of the microstructures during the two reheating processes at a temperature of 913 K. The traditional reheating microstructures are shown in Fig. 9 (a1) , (b1), and (c1), while the two-stage microstructures, with the first reheating at T_S = 855K for 5min are shown in Fig. 9 (a2), (b2), and (c2).

When the temperature is increased to 913 K, the grains become coarse and irregular, and intragranular liquid droplets (marked as ‘I’ in Fig. 7-9) can be found in the microstructure as the holding time is increased. As shown in Fig. 9 (a1), the traditional reheating microstructure still includes rosette morphology and a large amount of tiny entrapped liquid, but the grain boundary is now much clearer than it was at low temperature. The grain size of the two-stage reheating microstructure, seen in Fig. 9 (a2), is heterogeneous with coarsening and agglomeration of the solid grains. When the holding time is 25 min, the grain shape of the microstructure formed by the traditional reheating method, Fig. 9 (b1), is obviously irregular. In Fig. 9 (b2), a few liquid aggregations obviously occur at the multi-grain boundaries. Additionally, some small grains are found in the microstructure of two-stage reheating process. With further increasing holding time, large drops of liquid entrapped inside the solid grains are clearly noted in the semi-solid microstructures. At this point, the number of

intergranular droplets decreases, while their mean size increases because the small intragranular droplets gradually merge into larger ones by coalescence. The presence of small needle-like Mg_2Si precipitates and other insoluble compositions, such as Cr and Fe, are also observed at the grain boundary in Figs. 9 (c1) and (c2). These precipitates accumulate at the boundaries, impede the diffusion of liquid and inhibit the migration of the liquid film, which results in liquid segregation. Microstructure homogeneity is greatly affected by the severely coarsened grains and large regions of liquid segregation. These characteristics are likely to be unsuitable for the thixoforming processes because they may be detrimental to the thixotropic behavior of the semisolid billet, as shown in Fig. 9 (c1) and (c2).

The equivalent diameter, roundness and coarsening rate constant of the solid grains are analyzed with variation of holding time (i.e., 20, 25, and 30 min) at 903 K by comparing the traditional and two-stage reheating microstructures. The non-entrapped liquid ratio representing the possibility of defect occurrence is also considered, as shown in Fig. 10. The high non-entrapped liquid ratio may cause the occurrence of defects, such as shrinkage, during solidification.

The microstructure formed by the two-stage reheating, with the equivalent diameters of 112,124, and 137 μm at 903 K is finer than the microstructures formed by the traditional reheating process, with the equivalent diameters of 128,129, and 152 μm. The roundness of the grain shape at 903 K under different holding times during the two-stage reheating process was 0.80, 0.89, and 0.92, which is closer to 1 than the roundness produced by the traditional reheating 0.68, 0.77, and 0.90. If the solid grains are not sufficiently round, the grains will interfere with each other when sheared, leading to the disappearance of thixotropic behavior [19]. The grain coarsening is less obvious and the possibility of defect formation caused by the entrapped liquid is reduced for the two-stage reheating microstructure compared to that of traditional process, as shown in Fig. 10.

Equivalent diameter, roundness, coarsening rate constant and non-entrapped liquid ratio of solid grains are plotted versus temperature (i.e., 893, 903, and 913 K) at a holding time of 25 min in Fig. 11. The traditional and two-stage reheating microstructures are compared. The two-stage reheating microstructure (with equivalent diameter s of 131,124, and 122 μm) is finer than the traditional reheating microstructure (with diameters of 146,129, and 124 μm). The low temperature results

in low interfacial energy, and the microstructure retains its irregular rosette shape. With increasing reheating temperature, coarsening tends to occur through coalescence and Ostwald ripening. The equivalent diameter of solid grains at a reheating temperature of 913 K is a little lower than that of the solid grains reheated at 903 K, which implies that Ostwald ripening dominates in the coarsening of grains; small grains disappear gradually in favor of bigger solid grains by diffusion. The slight decreasing of roundness and coarsening rate constant also suggest the occurrence of Ostwald ripening. These grain shape factors have to be balanced with considerations of the reheating temperature. The roundness of the solid grains at a holding time of 25min under different reheating temperatures (i.e., 893, 903, and 913 K) during the two-stage reheating process is 0.69, 0.89 and 0.84; these values are closer to 1 than the values (i.e. 0.60, 0.77, and 0.72) during the traditional reheating process. Coarsening is less obvious in the two-stage reheating microstructure compared to that formed by the traditional process. The low non-entrapped liquid ratio may reduce the occurrence of defect formation during solidification.

Overall, the microstructural evolution during the reheating process includes two mechanisms: (1) the coalescence of solid grains, and (2) Ostwald ripening. Concerning (1), some solid grains remain irregularly shaped and are polyhedral in spite of extending the holding time, which is possibly caused by low angle or low interfacial energy of the unwetted grain boundaries [20]. These partially unwetted boundaries or the initial stages of coalescence are summarized as “A” in Fig. 6-8. With increased temperature and time, the grain growth also exhibits coarsening (marked as “C”) or big coalescence of several adjacent grains (as indicated by “O”). Coalescence between two adjacent grains that share the same boundaries are classified by a two-way arrow. Meanwhile, some intragranular liquid droplets can also be observed in the microstructure, labelled as “I”. Concerning (2), the finest solid particles melt because of their high curvatures, which help with the formation of the larger ones [20-21]. As indicated in Fig. 6-8, the one-way arrow shows the direction of the accumulation of small solid grains, resulting in a slight decrease in the equivalent diameters and the coarsening rate constant.

4. Conclusions

(1) Evolutions of the microstructures of the 6061 wrought aluminum alloy have been investigated, under both traditional and two-stage reheating processes. The

optimal two-stage reheating process for the 6061 wrought aluminum alloy is as follows: in an electrical resistance furnace, the samples are held at the solidus temperature T_S for 5 min, and then heated to the desirable temperature at an average heating rate of 10 K/min.

(2) A desirable semi-solid microstructure with fine and uniform spheroidal grains is obtained using this preferred two-stage reheating process. The obtained microstructure is comprised of fine and spheroidal grains and homogeneously distributed liquid phase along the grain boundaries.

(3) The microstructural characteristics of the 6061 wrought aluminum alloy formed by the traditional and two-stage reheating process are considered under different conditions, with temperatures from 893 to 913 K and holding times of 20, 25 and 30min. In general, the equivalent diameter is much finer, the grain shape is more rounded, coarsening is less obvious, and the possibility of defects caused by entrapped liquid is lower for the two-stage reheating microstructure as compared to those of the traditional method.

This work was supported by the National Natural Science Foundation Project of China (51374109).

5. References

[1] J. Jiang, Y. Wang, J. Qu, Z. Du, Y. Sun, S. Luo: *J. Alloy Compd.*, 2010, *vol.*497, *pp.* 62-7.

[2] G.C. Gu, R. Pesci, L. Langlois, E. Becker, R. Bigot, M.X. Guo: *Acta. Mater.*, 2014, *vol.*66, *pp.* 118-31.

[3] S. Terzi, M. Rappaz, J.M. Drezet, M. Rappaz: *Acta. Mater.*, 2013, *vol.* 61, *pp.*3831-41.

[4] R. Canyook, J. Wannasin, S. Wisuthmethangkul, M.C. Flemings: *Acta. Mater.*, 2012, *vol.*60, *pp.* 3501-10.

[5] M. Sistaninia, A.B. Phillion, J.M. Drezet, M. Rappaz: *Acta. Mater.*, 2012, *vol.* 60, *pp.* 3902-11.

[6] S. Chayong, H.V. Atkinson, P. Kapranos: *Mater. Sci. Eng. A*, 2005, *vol.* 390, *pp.* 3-12.

[7] H.V. Atkinson, D. Liu: *Mater. Sci. Eng. A,* 2008, *vol.* 496, *pp.*439-46.

[8] N. Haghdadi, A. Zarei-Hanzaki, S. Heshmati-Manesh, H.R. Abedi, S.B. Hassas-Irani: *Mater. Design,* 2013, *vol.*49, *pp.* 878.

[9] J. Jiang, Y. Wang, H.V. Atkinson: *Mater. Charact.,* 2014, *vol.* 90, *pp.*52-61.

[10] P.K. Seo, C.G. Kang: *J. Mater. Process Tech.,* 2005, *vol.* 162, *pp.* 402-9.

[11] M. Moradi, M. Nili-Ahmadabadi, B. Poorganji, B. Heidarian, M.H. Parsa, T. Furuhara: *Mater. Sci. Eng. A,* 2010, *vol.* 527, *pp.* 4113-21.

[12] H.V. Atkinson, D. Liu: *Mater. Sci. Eng. A,* 2008, *vol.* 496, *pp.* 439-46.

[13] A. Bolouri, M. Shahmiri, C.G. Kang: *J. Mater. Sci.*, 2012, *vol.* 47, *pp.* 3544-53.

[14] E. Tzimas, A. Zavaliangos: *Mater. Sci. Eng. A,* 2000, *vol.* 289, *pp.* 228-40.

[15] S. Annavarapu, R.D. Doherty: *Acta. Mater.,* 1995, *vol.* 43, *pp.* 3207-30.

[16] Z. Wang, Z. Ji, M. Hu, H. Xu: *Mater. Charact.,* 2011, *vol.* 62, *pp.* 925-30.

[17] A. Bolouri, M. Shahmiri, E.N.H. Cheshmeh: *T. Nonferr. Metal Soc.,* 2010, *vol.* 20(9) , *pp.* 1663-1671.

[18] A. Neag, V. Favier, R. Bigot, M. Pop: *J. mater. Process Tech.,* 2012, *vol.* 212, *pp.* 1472-80.

[19] S. Ji, Z. Fan, M.J. Bevis: *Mater. Sci. Eng. A,* 2001, *vol.* 299, *pp.* 210-7.

[20] S. Luo, Q. Chen, Z. Zhao: *Mater. Sci. Eng. A,* 2009, *vol.* 501, *pp.*146-52.

[21] H.V. Atkinson, K. Burke, G. Vaneetveld: *Mater. Sci. Eng. A,* 2008, *vol.* 490, *pp.*266-76.

Table 1 Chemical composition of the 6061 aluminum alloy (mass fraction, %)

	Si	Mg	Cu	Cr	Fe	Zn	Sn	Ga	Al
6061	1.36	1.20	0.493	0.314	0.139	0.0449	0.0379	0.0123	balance

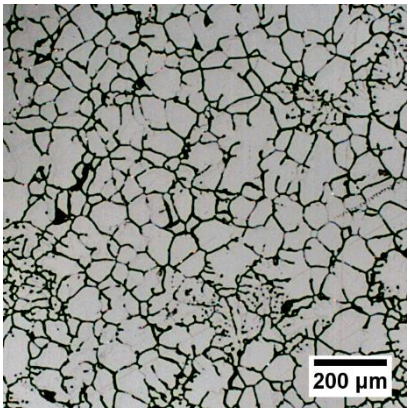

Fig. 1 The non-dentritic microstructure of the 6061wrought aluminum alloy obtained by near-liquidus semi-continuous casting

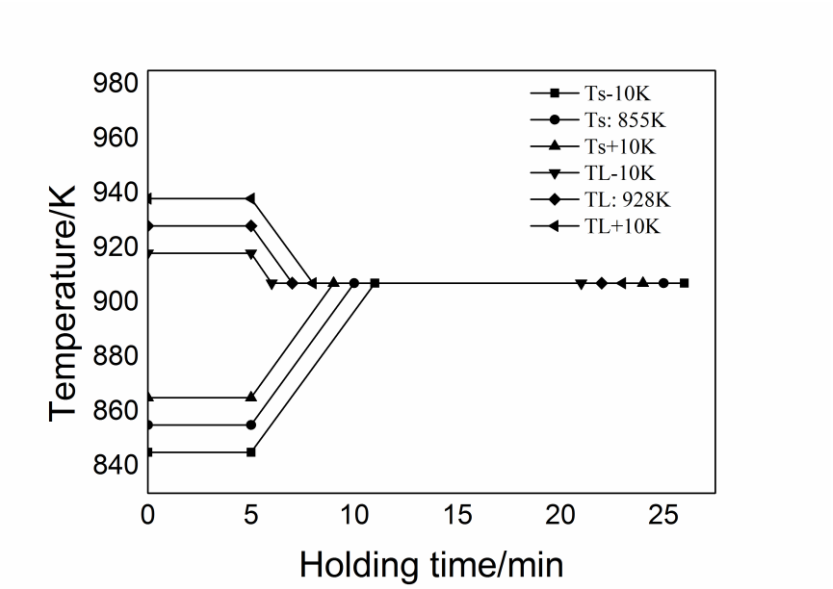

Fig. 2 Research scheme of the reheating process of thixotropic billets for the 6061wrought aluminum alloy

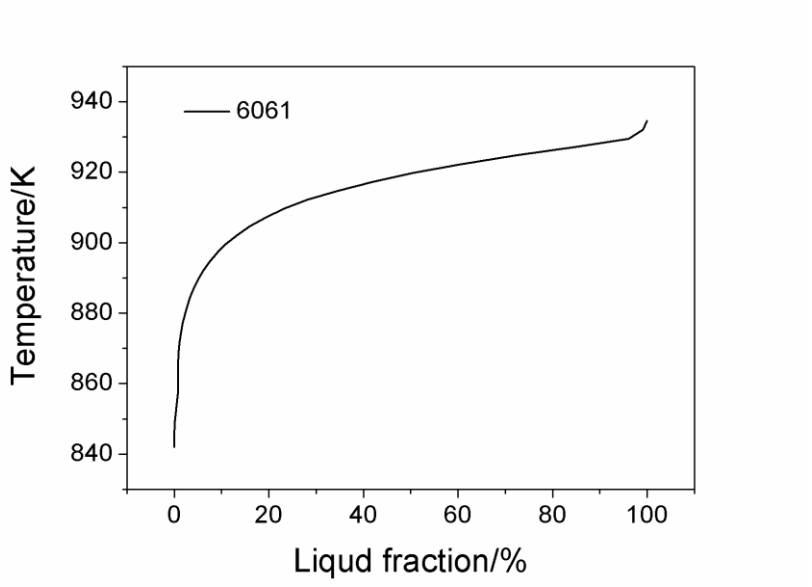

Fig. 3 The liquid fraction as a function of temperature obtained from DSC

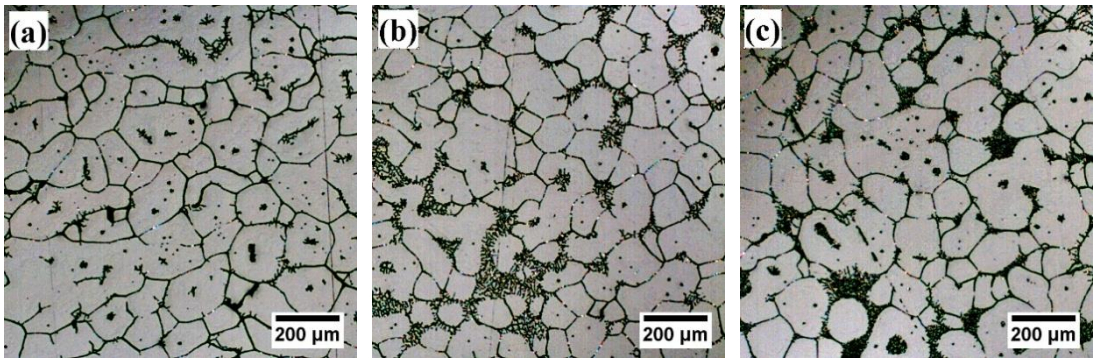

Fig. 4 Microstructure of the 6061 alloy obtained from two-stage reheating process near the solidus temperatures: (a) 845-907 K, (b) 855 -907 K, and (c) 865-907K

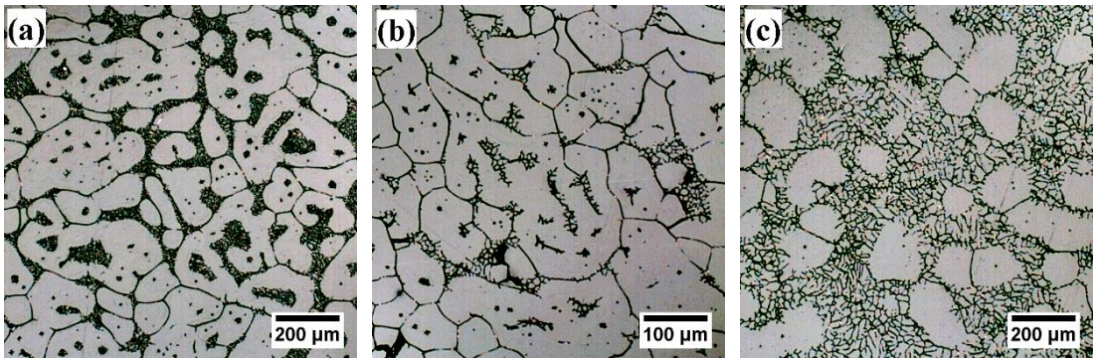

Fig. 5 Microstructure of the 6061 alloy obtained from two-stage reheating process near the liquidus temperatures: (a) 918-907 K, (b) 928 -907 K, and (c) 938-907K

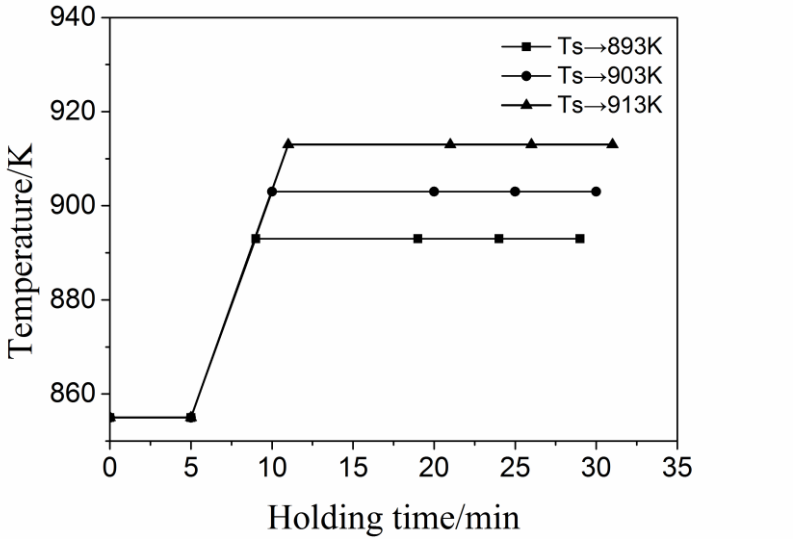

Fig. 6 The optimal two-stage reheating process for the 6061wrought aluminum alloy

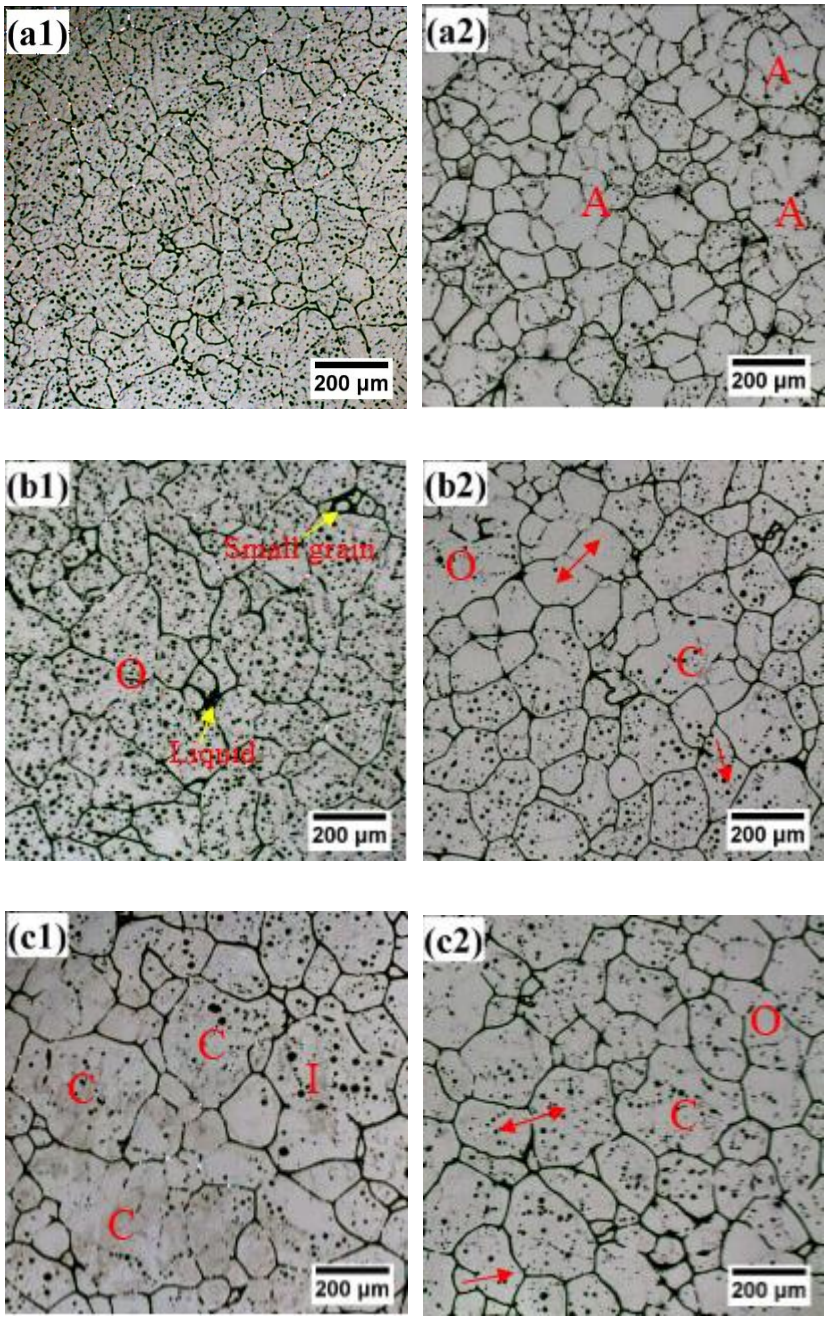

Fig. 7 Comparable microstructures of 6061 alloy obtained from the traditional (a1, b1, c1) and the two-stage (a2, b2, c2) reheating processes at 893 K holding for: (a) 20 min, (b) 25 min, and (c) 30 min

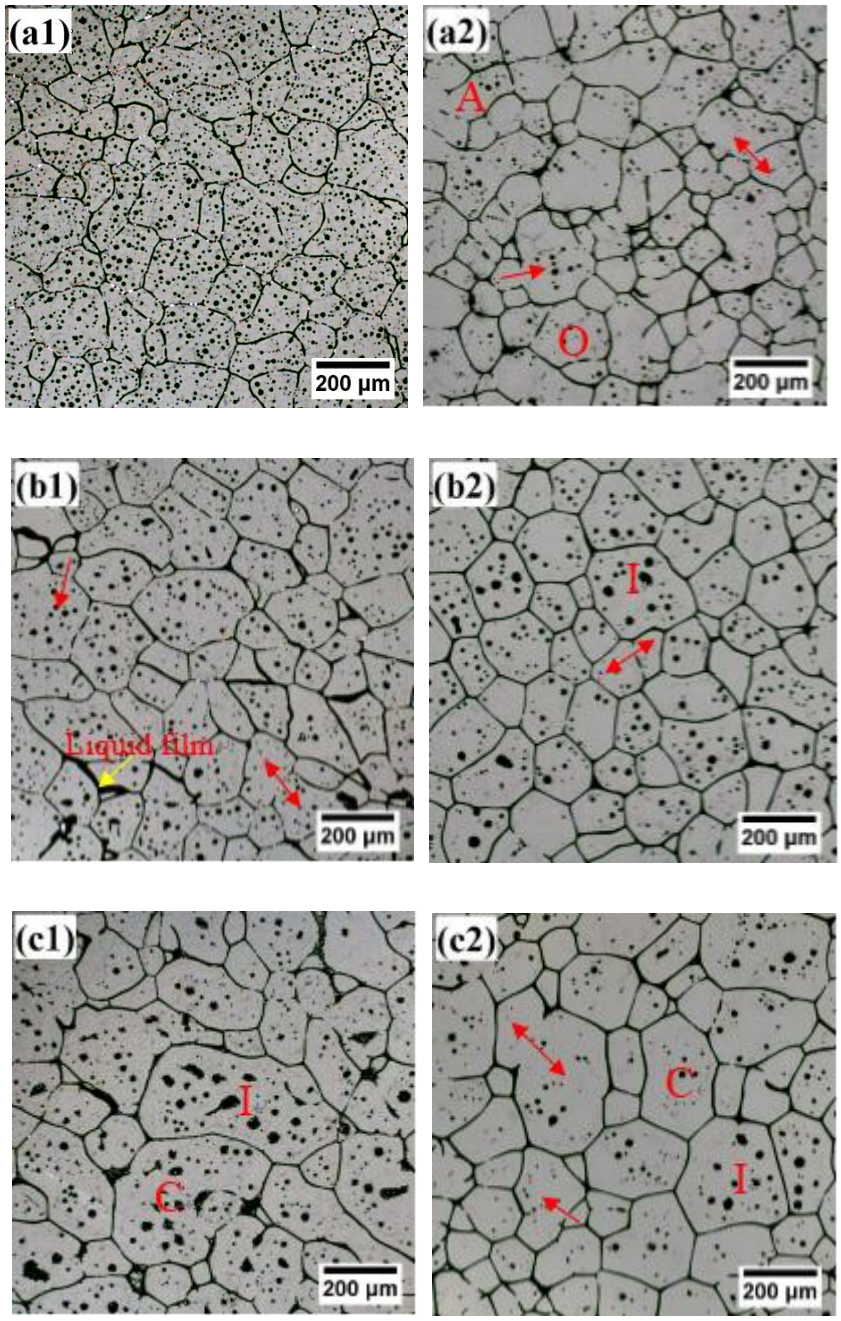

Fig. 8 Comparable microstructures of 6061 alloy obtained from the traditional (a1, b1, c1) and the two-stage (a2, b2, c2) reheating process at 903 K holding for: (a) 20 min, (b) 25 min, and (c) 30 min

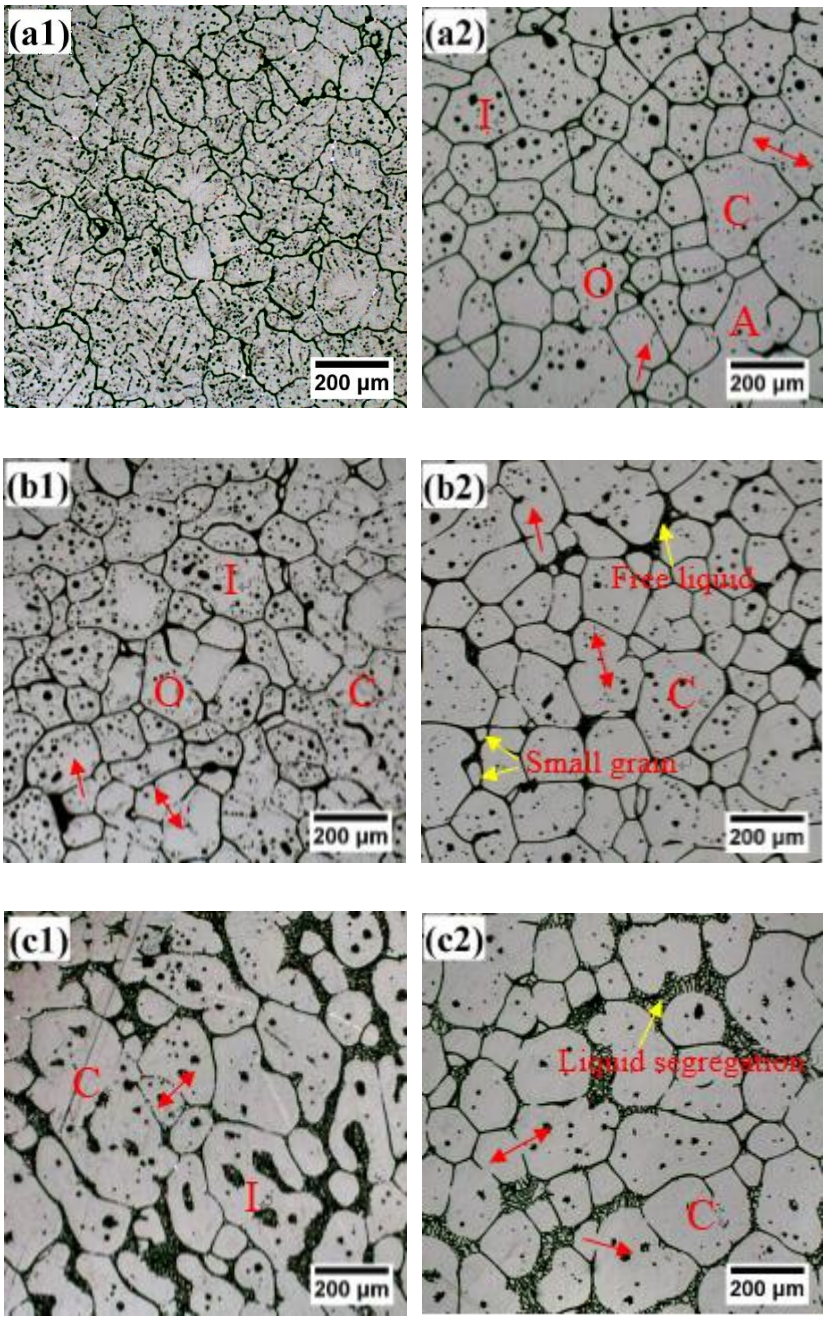

Fig. 9 Comparable microstructures of 6061 alloy obtained from the traditional (a1, b1, c1) and the two-stage (a2, b2, c2) reheating process at 913K holding for: (a) 20 min, (b) 25 min, and (c) 30 min

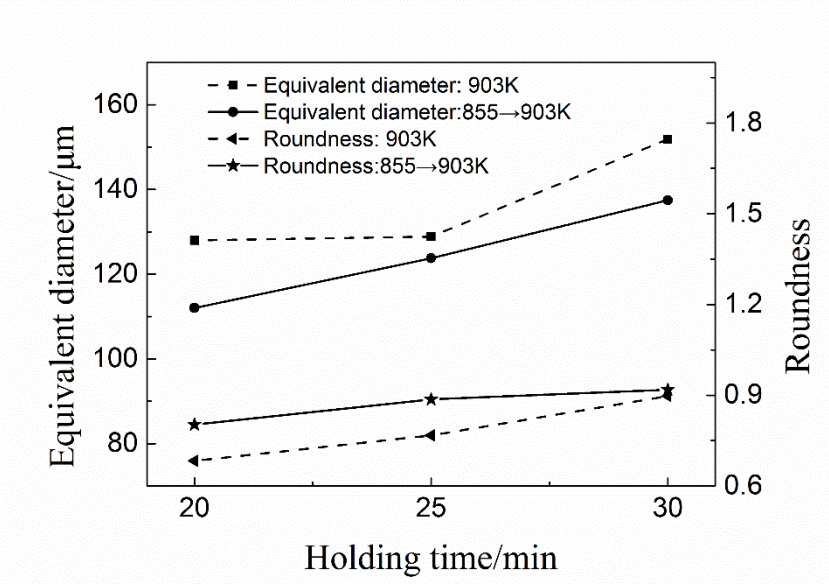

(a)

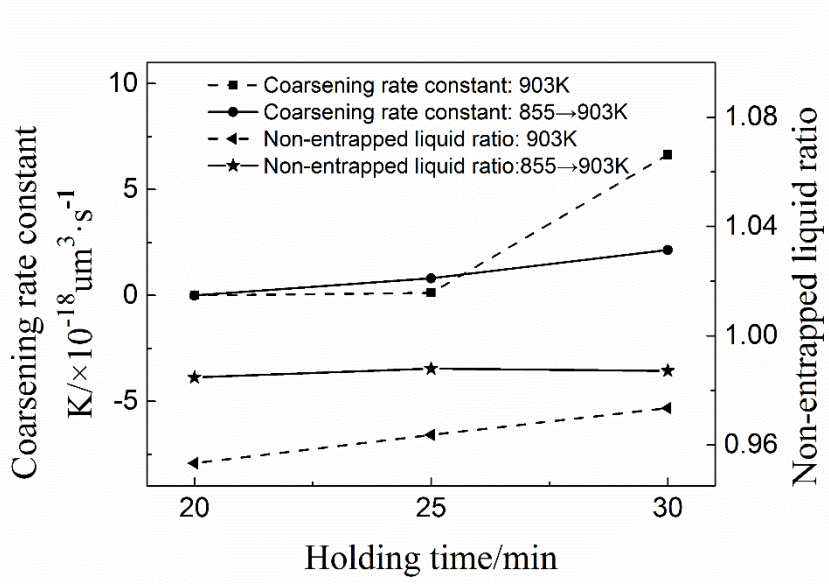

(b)

Fig. 10 Dependence of (a) the equivalent diameter, and roundness, and (b) coarsening rate constant and non-entrapped liquid ratio on the holding time at a temperature of 903K for both the traditional and two-stage reheating process for the 6061 alloy

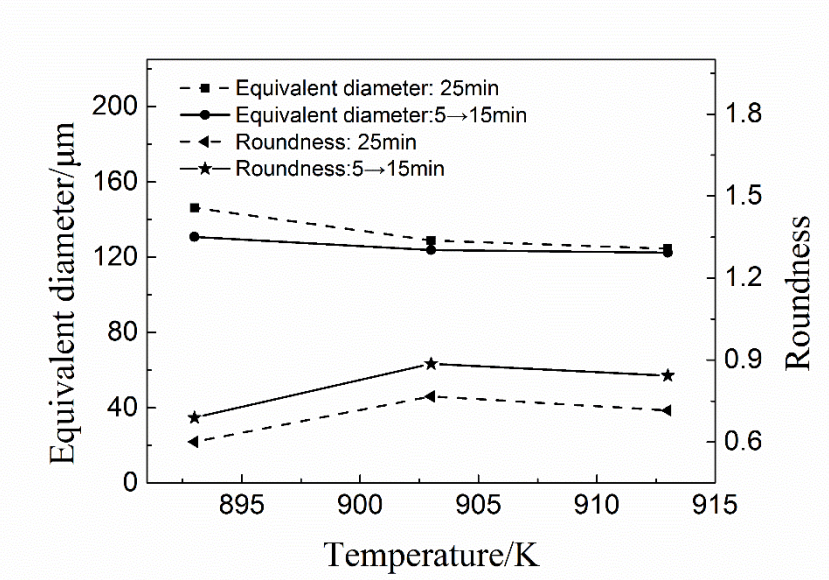

(a)

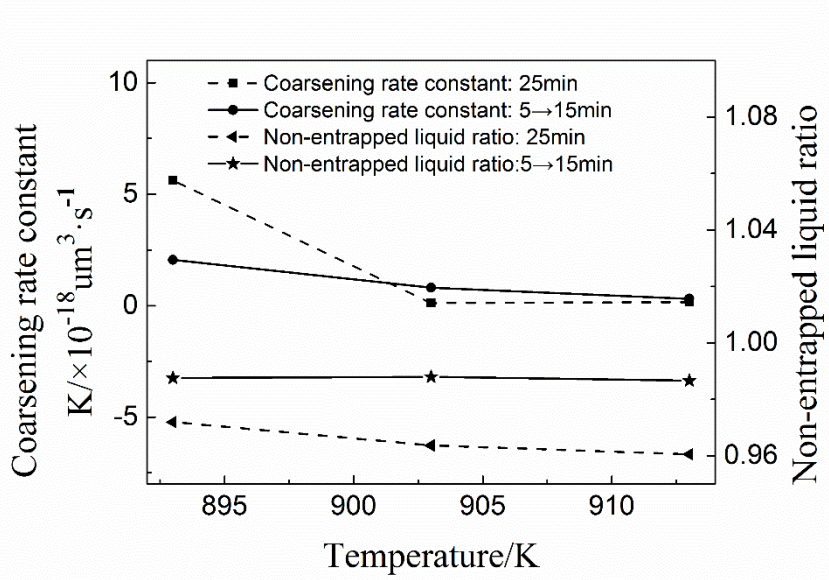

(b)

Fig. 11 Dependence of (a) the equivalent diameter and roundness, (b) the coarsening rate constant and non-entrapped liquid ratio on the temperatures at a holding time of 25min during both traditional and two-stage reheating processes for the 6061 alloy